



Dispersion-enhanced tunability of the laser-frequency response to the cavity-length change

Savannah L. Cuozzo  and Eugeny E. Mikhailov*

Department of Physics, College of William & Mary, Williamsburg, Virginia 23187, USA

 (Received 19 December 2018; revised manuscript received 8 March 2019; published 27 August 2019)

We report on the controllable response of the lasing frequency to the cavity round-trip path change. This is achieved by modifying the dispersion of the intracavity medium in the four-wave mixing regime in Rb. We can either increase the response by at least a factor of 2.7 or drastically reduce it. The former regime is useful for sensitive measurements tracking the cavity round-trip length and the latter regime is useful for precision metrology.

DOI: [10.1103/PhysRevA.100.023846](https://doi.org/10.1103/PhysRevA.100.023846)

I. INTRODUCTION

We control the response of the lasing frequency to the laser cavity-length change on demand—allowing for either dramatic enhancement or suppression. The resonant frequency link to the cavity round-trip path is the foundation for optical precision measurements such as displacement tracking, temperature sensing, optical rotation tracking [1], gravitational wave sensing [2], and refractive index change sensing [3]. In other applications, the laser provides a stable frequency reference, such as precision interferometry [4], optical atomic clocks [5], and distance ranging [6], where the response of the lasing frequency to the cavity path length change should be reduced. Our findings allow for improved laser-assisted precision metrology and potential to make lasers less bulky and immune to the environmental changes in real-world applications.

II. THEORETICAL DESCRIPTION

The addition of a dispersive medium to a cavity modifies its frequency response [7] to the geometrical path change (dp) according to

$$df_d = -\frac{n}{n_g} \frac{dp}{p_{\text{tot}}} f_0, \quad (1)$$

where f_0 is the original resonant frequency, $p_{\text{tot}} = p_e + p_d n$ is the total optical round-trip path of the cavity, p_d is the length of the dispersive element, p_e is the length of the empty (nondispersive) part of the cavity, n is the refractive index, and n_g is the generalized refractive group index given by

$$n_g = n + \frac{np_d}{p_{\text{tot}}} f_0 \frac{\partial n}{\partial f}. \quad (2)$$

We define the pulling factor (PF) as the ratio of dispersive to empty (nondispersive, $n_g = n$) cavity response for the same path change:

$$\text{PF} \equiv \frac{df_d}{df_e} = \frac{n}{n_g}. \quad (3)$$

The PF is the figure of merit for the enhancement of the cavity response relative to *canonical* lasers or passive cavities operating in the weak dispersion regime with $n_g = n$.

We tune the PF in the range from -0.3 to at least 2.7 ± 0.4 (see Fig. 1), by tailoring the refractive index of our lasing medium. This is the first demonstration of high and tunable PF in the laser. We can also push our system response further and reach the bifurcating regime.

Because of the Kramers-Kronig relationship, the negative dispersion is accompanied by local absorption, so it is not surprising that so far the $\text{PF} > 1$ regime was experimentally demonstrated only in passive, nonlasing cavities [8–10] with $\text{PF} = 363$. For active cavities, Yablon *et al.* [11] *inferred* a $\text{PF} \sim 190$ via analysis of the lasing linewidth. The increased stability regime ($\text{PF} < 1$) was demonstrated in lasing [12] cavities with the smallest PF being $1/663$ [13]. Superradiant (“bad-cavity”) lasers, where an atomic gain line is much narrower than a cavity linewidth, exhibit ultralow $\text{PF} < 10^{-6}$ [14,15]. Our empty cavity linewidth is about 13 MHz, which is larger than any atomic decoherence time, so we operate in the “bad-cavity” regime. However, unlike previously reported work in [14,15], we can also achieve higher than one PF.

Similar to Ref. [16], we present a simple model of the transmission or amplification spectral line where the index of refraction has the dependence:

$$n(f) = 1 + \epsilon \frac{\gamma \Delta f}{\Delta f^2 + \gamma^2}, \quad (4)$$

where ϵ is the resonance strength, Δf is the detuning from the medium resonance frequency (f_m), and γ is the resonance width, since $n(f) - 1 \ll 10^{-5}$ for a vapor-filled cavity. For transmission or gain resonances with $\epsilon > 0$, the minimum and maximum PF are

$$\text{PF}_{\text{max}} = \frac{1}{1 - \epsilon/\epsilon_{\text{th}}} \quad \text{at} \quad \Delta f = \pm\sqrt{3}\gamma, \quad (5)$$

$$\text{PF}_{\text{min}} = \frac{1}{1 + 8\epsilon/\epsilon_{\text{th}}} \quad \text{at} \quad \Delta f = 0, \quad (6)$$

where

$$\epsilon_{\text{th}} = \frac{8\gamma}{f_m} \frac{p_{\text{tot}}}{p_d} \quad (7)$$

is the bifurcating threshold resonance strength.

*eemikh@wm.edu

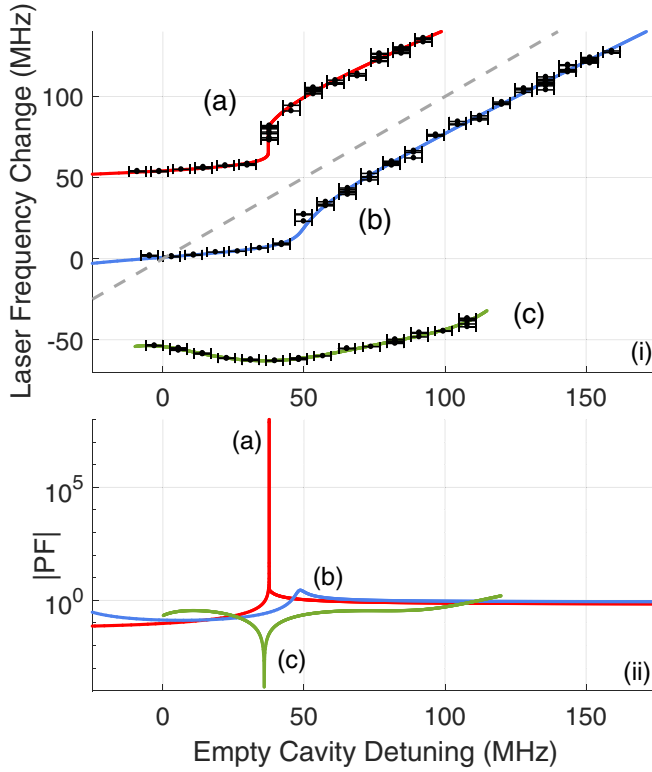


FIG. 1. (i) The experimental lasing-frequency dependence on empty cavity detuning (round-trip path change) in (a) bifurcating regime with estimated ultrahigh PF $> 10^8$, (b) high pulling regime with PF = 2.7 ± 0.4 , and (c) enhanced stability regime where $|PF| < 0.2$ crossing 0. The solid lines [(a) and (b)] show our best fits of the laser frequency dependence using the model described by Eq. (4); the (c) line is the polynomial fit of the fifth degree. The straight dashed line shows the PF = 1 dependence (i.e., for an empty cavity). (ii) The PF calculated based on the fits presented in panel (i).

III. ANALYSIS

The analysis of the dispersion [Eq. (4)] and its influence on the resonant frequency of the cavity and PF is shown in Fig. 2. As expected, the amplification line has positive dispersion on resonance [see Fig. 2(a)]. Positive dispersion is associated with a large and positive group index, which results in weak dependence (low pulling factor) of the lasing frequency on the cavity path change (empty cavity detuning), as shown in Fig. 2(b). Away from resonance, the dispersion is negative, leading to high PFs, as shown in Fig. 2(b). As the amplification (ϵ) increases, the PF_{\min} becomes smaller at the center of the resonance, as shown in Fig. 2(b). Consequently, the PF_{\max} continuously grows and reaches infinity at $\epsilon = \epsilon_{\text{th}}$ where the resonant frequency bifurcates [see Fig. 2(b)].

To track dependence of the cavity resonant frequency on the cavity path length, we solve

$$p_{\text{tot}} = m \frac{c}{f_d}, \quad (8)$$

where m is the fixed mode number and c is the speed of light in vacuum. In experiments, it is easier to track the empty cavity detuning (i.e., resonance frequency change, Δf_e), which is directly linked to the cavity-path change via Eq. (1) with $n_g = n$. The resulting dependencies are shown in Fig. 2(c).

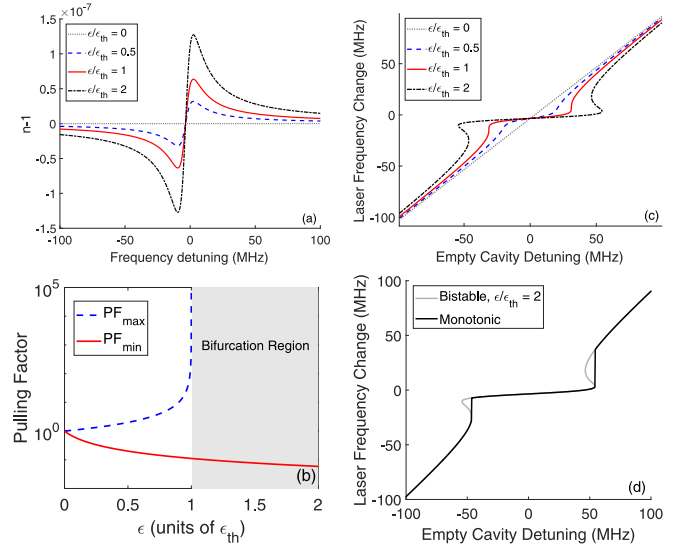


FIG. 2. (a) Refractive index change ($n - 1$), (b) dependence of maximum and minimal achievable PF on resonance strength, (c) laser frequency change, and (d) bifurcating behavior as functions of detuning (or cavity path change). For all figures, γ is set to 6 MHz.

If the negative dispersion is strong enough, the group index could be negative. This would lead to negative PF and to negative dependence of the lasing frequency on the cavity detuning [see the line corresponding to $\epsilon = 2\epsilon_{\text{th}}$ in Fig. 2(c)]. This behavior is nonphysical, since it corresponds to a bifurcation [16]: Multiple lasing frequencies for the same cavity detuning. Consequently, the laser would “jump” to avoid the negative PF region and preserve the monotonic behavior, as shown in Fig. 2(d) and experimentally in Fig. 1(i)a.

The most important conclusion from the amplifying line analysis is that high-pulling (response-enhancement) regions exist slightly away from the *gain* resonance. The precursor of such a regime is a reduced PF region in close vicinity to the resonance. The off-resonance behavior was overlooked in the literature, while it actually provides the road to high PF. Away from the amplification resonance, the system still has enough gain to sustain lasing, and yet it still has large negative dispersion [see Fig. 2(a)]. As detuning from the resonance increases, the dispersion becomes negligible, PF approaches unity [see Fig. 2(c) and experimental data in Figs. 1(a) and 1(b)], amplification drops, and eventually lasing ceases.

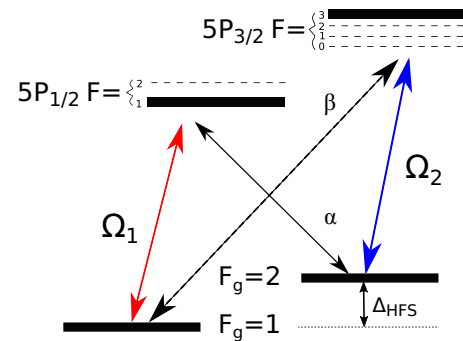


FIG. 3. Schematic diagram of interacting light fields and relevant ^{87}Rb levels.

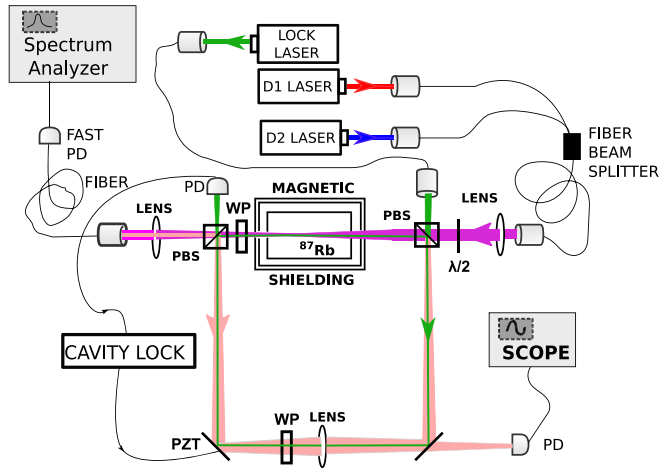


FIG. 4. Schematic diagram of the setup. PD, photo detector; WP, wave plate; $\lambda/2$, half-wavelength wave plate; PBS, polarizing beam splitter; and PZT, piezoelectric transducer.

IV. METHODS

To experimentally demonstrate the modified lasing response to the cavity path change, one needs a narrow gain line to achieve the highest positive dispersion. We utilized the N -level pumping scheme depicted in Fig. 3. The theory and preliminary experimental study of this arrangement are covered in Refs. [12,17,18]. The strong pumping field Ω_1 creates a transmission line for the field α due to electromagnetically induced transparency. However, the Ω_1 field alone is not enough to create the amplification. To create the gain for the α field, we apply another strong repumping field (Ω_2). There is also gain for the β field, which completes the four-wave mixing arrangement of fields Ω_1 , Ω_2 , α , and β . But the cavity is tuned to sustain lasing only for α .

Our lasing cavity is similar to the one used in Ref. [12]. The ring cavity is made of two polarizing beam splitters (PBS) and two flat mirrors, as seen in Fig. 4. The round trip path of the cavity is 80 cm. A 22-mm-long Pyrex cylindrical cell with antireflection coatings on its windows is placed between the two PBSs and filled with isotopically pure ^{87}Rb . The cell is encased in a three-layer magnetic shield and its temperature is set to 100°C . The optical stability of the cavity is increased by adding a 30-cm-focal-length lens placed between the two mirrors. This lens also places the cavity's mode waist inside the ^{87}Rb cell.

To produce experimental data sets (a) and (b) shown in Fig. 1, two pump lasers are tuned near D1 (795 nm) and D2 (780 nm), corresponding to Ω_1 and Ω_2 fields in Fig. 3. The pump fields are coupled to a fiber beam splitter and amplified by a solid-state tapered amplifier to powers ranging between 100 mW for set (a) and 170 mW for set (b), and then injected into a ring cavity through a polarizing beam splitter (PBS). The D1 laser is tuned 700 MHz below the $5S_{1/2}F_g = 1 \rightarrow 5P_{1/2}F = 1$ transition, and D2 is set to 500 MHz below the $5S_{1/2}F_g = 2 \rightarrow 5P_{3/2}F = 3^{87}\text{Rb}$ transition, as seen in Fig. 3. They provide amplification for fields α and β , which are generated orthogonal to pump field polarization. Only the α field resonantly circulates in the

cavity, since the pumps exit the cavity via the second PBS and β is kept off resonance with the cavity.

Since the D1 pump laser is fixed, the beat note of the pump (Ω_1) and the lasing field (α) with its frequency close to ^{87}Rb hyperfine splitting ($\Delta_{\text{HFS}} \approx 6.8\text{ GHz}$) is related to the frequency of the ring cavity laser and allows us to monitor the dispersive laser frequency change (Δf_d). We control the cavity length by locking it to an auxiliary laser (called the lock laser) with a wavelength of 795 nm that is far detuned from any atomic resonances and senses a “would be empty” (dispersion-free) cavity detuning (Δf_e). This lock laser beam counterpropagates relative to the pump beams and the lasing field to avoid contaminating the detectors monitoring the ring cavity lasing. Two wave plates (WP) are placed inside the cavity. One is to spoil polarization of the lock field and allow it to circulate in the cavity. The other rotates the lasing field polarization by a small amount. This allows it to exit the cavity and mix in with the pump field on the fast photodetector.

V. RESULTS

The maximum response has the lower bound of $\text{PF}_{\text{max}} = 1.1 \times 10^8$ at the 90% confidence level for the data set (a), shown in Fig. 1. The upper bound for PF_{max} is infinity since the data set belongs to the bifurcating regime. However, one can smoothly approach this limit by carefully controlling the cavity detuning, as our analysis shows in Fig. 1(ii)a. The PF_{min} range is (0.08 to 0.10) for this data set.

We can avoid bifurcation by increasing the pumps' powers (i.e., we increase γ via power broadening), as shown in the data set (b) of Fig. 1. This data demonstrates PF_{max} in the range (2.3 to 3.2). Also, the range of detuning with $\text{PF} > 1$ is wider. To estimate confidence bounds, we use the modified smoothed bootstrap method [19].

We are able to make our dispersive laser insensitive to its path change, as shown in data set (c) of Fig. 1. We tune the D1 laser to 400 MHz above the $5S_{1/2}F_g = 1 \rightarrow 5P_{1/2}F = 1$ transition and keep D2 at 500 MHz below the $5S_{1/2}F_g = 2 \rightarrow 5P_{3/2}F = 3^{87}\text{Rb}$ transition, while maintaining combined pump power at 95 mW. Assuming a smooth dependence on the empty cavity detuning, the PF at the bottom of the U-like curve is exactly zero, as the laser frequency decreases and then increases, while the cavity path (the auxiliary laser detuning) changes monotonically. Our model governed by Eq. (4) cannot explain the arching behavior, since it does not account for the dependence of the dispersion on the lasing power. However, a more complete model which solves density matrix equations of the N -level scheme predicted such a possibility [12].

VI. CONCLUSION

There is ongoing debate of whether the modified cavity response leads to improved sensitivity (signal-to-noise ratio) of path-change-sensitive detectors. However, laser-based sensors in certain applications might benefit either from enhanced $\text{PF} > 1$ (for example, gyroscopes [7]) or reduced $\text{PF} < 1$, since sensitivity, i.e., the ratio of the response to the lasing linewidth (uncertainty), scales as $1/\text{PF}$ [14,20,21]. The

tunability and versatility of our system allows us to probe either case.

In conclusion, we achieved about 2.7 ± 0.4 increase of the laser response to the cavity-path-length change relative to canonical lasers. We also can significantly reduce the response, making our laser vibration insensitive. These findings broadly impact the fields of laser sensing and metrology, including laser ranging, laser gyroscopes, vibrometers, and laser frequency standards.

ACKNOWLEDGMENTS

E.E.M. and S.L.C. are thankful for the support of Virginia Space Grant Consortium provided by Grants No. 17-225-100527-010 and No. NNX15AI20H. We would like to thank M. Simons, O. Wolfe, and D. Kutzke for assembling the earlier prototype of our laser. We also thank S. Rochester and D. Budker for their earlier work on an N -level theoretical model.

-
- [1] W. W. Chow, J. Gea-Banacloche, L. M. Pedrotti, V. E. Sanders, W. Schleich, and M. O. Scully, *Rev. Mod. Phys.* **57**, 61 (1985).
 - [2] B. P. Abbott, R. Abbott, T. D. Abbott, M. R. Abernathy, F. Acernese, K. Ackley, C. Adams, T. Adams, P. Addesso, R. X. Adhikari *et al.* (LIGO Scientific Collaboration and Virgo Collaboration), *Phys. Rev. Lett.* **116**, 061102 (2016).
 - [3] J. Li, H. Niu, and Y. X. Niu, *Opt. Eng.* **56**, 050901 (2017).
 - [4] D. Martynov *et al.*, *Phys. Rev. D* **93**, 112004 (2016).
 - [5] A. D. Ludlow, M. M. Boyd, J. Ye, E. Peik, and P. O. Schmidt, *Rev. Mod. Phys.* **87**, 637 (2015).
 - [6] Y.-S. Jang and S.-W. Kim, *Int. J. Precis. Eng. Manuf.* **18**, 1881 (2017).
 - [7] M. S. Shahriar, G. S. Pati, R. Tripathi, V. Gopal, M. Messall, and K. Salit, *Phys. Rev. A* **75**, 053807 (2007).
 - [8] G. S. Pati, M. Salit, K. Salit, and M. S. Shahriar, *Phys. Rev. Lett.* **99**, 133601 (2007).
 - [9] D. D. Smith, H. A. Luckay, H. Chang, and K. Myneni, *Phys. Rev. A* **94**, 023828 (2016).
 - [10] D. D. Smith, H. Chang, P. F. Bertone, K. Myneni, L. M. Smith, and B. E. Grantham, *Opt. Express* **26**, 14905 (2018).
 - [11] J. Yablon, Z. Zhou, M. Zhou, Y. Wang, S. Tseng, and M. S. Shahriar, *Opt. Express* **24**, 27444 (2016).
 - [12] D. T. Kutzke, O. Wolfe, S. M. Rochester, D. Budker, I. Novikova, and E. E. Mikhailov, *Opt. Lett.* **42**, 2846 (2017).
 - [13] J. Yablon, Z. Zhou, N. Condon, D. Hileman, S. Tseng, and S. Shahriar, *Opt. Express* **25**, 30327 (2017).
 - [14] J. G. Bohnet, Z. Chen, J. M. Weiner, D. Meiser, M. J. Holland, and J. K. Thompson, *Nature (London)* **484**, 78 (2012).
 - [15] M. A. Norcia, J. R. K. Cline, J. A. Muniz, J. M. Robinson, R. B. Hutson, A. Goban, G. E. Marti, J. Ye, and J. K. Thompson, *Phys. Rev. X* **8**, 021036 (2018).
 - [16] Z. Zhou, J. Yablon, M. Zhou, Y. Wang, A. Heifetz, and M. Shahriar, *Opt. Commun.* **358**, 6 (2016).
 - [17] E. E. Mikhailov, J. Evans, D. Budker, S. M. Rochester, and I. Novikova, *Opt. Eng.* **53**, 102709 (2014).
 - [18] N. B. Phillips, I. Novikova, E. E. Mikhailov, D. Budker, and S. Rochester, *J. Mod. Opt.* **60**, 64 (2013).
 - [19] B. Efron and R. J. Tibshirani, *An Introduction to the Bootstrap* (Chapman and Hall, 1994).
 - [20] S. J. M. Kuppens, M. P. van Exter, and J. P. Woerdman, *Phys. Rev. Lett.* **72**, 3815 (1994).
 - [21] C. Henry, *IEEE J. Quantum Electron.* **18**, 259 (1982).